

- <sup>1</sup>L. M. Biberman, Zh. Eksp. Teor. Fiz. 17, 416 (1947).  
<sup>2</sup>T. Holstein, Phys. Rev. 72, 1212 (1947); 83, 1159 (1951).  
<sup>3</sup>K. F. Renk and J. Peckenzell, J. Phys. (Paris) 33, Suppl. C4, 103 (1972).  
<sup>4</sup>K. F. Renk and J. Deisenhofer, Phys. Rev. Lett. 26, 764 (1971).  
<sup>5</sup>A. A. Kaplyanskiĭ, S. A. Basun, V. A. Rachin, and R. A. Titov, Pis'ma Zh. Eksp. Teor. Fiz. 21, 438 (1975) [JETP Lett. 21, 200 (1975)]; Pis'ma Zh. Tekh. Fiz. 1, 628 (1975) [Sov. Tech. Phys. Lett. 1, 281 (1975)]; Fiz. Tverd. Tela (Leningrad) 17, 3661 (1975) Sov. Phys. Solid State 17, 2380 (1975); Akust. Zh. 22, 599 (1976) [Sov. Phys. Acoust. 22, 333 (1976)].  
<sup>6</sup>J. I. Dijkhuis, A. van der Pol, and H. W. de Wijn, Phys. Rev. Lett. 37, 1554 (1976).  
<sup>7</sup>R. S. Meltzer and J. E. Rives, Phys. Rev. Lett. 38, 421 (1977).  
<sup>8</sup>Yu. A. Vdovin and V. M. Galitskiĭ, Zh. Eksp. Teor. Fiz. 48, 1352 (1965) [Sov. Phys. JETP 21, 904 (1965)].  
<sup>9</sup>Yu. A. Vdovin, Zh. Eksp. Teor. Fiz. 50, 395 (1966) [Sov. Phys. JETP 23, 263 (1966)].  
<sup>10</sup>V. M. Ermachenko, Zh. Eksp. Teor. Fiz. 51, 1833 (1966) [Sov. Phys. JETP 24, 1236 (1967)].  
<sup>11</sup>A. I. Alekseev, in: Vzaĭmodeĭstviya izlucheniya s veshchestvom (Interaction of Radiation with Matter), ed. A. I. Alekseev, Atomizdat, 1966, p. 70.  
<sup>12</sup>Yu. A. Vdovin and V. M. Ermachenko, *ibid.*, p. 89.  
<sup>13</sup>Yu. A. Vdovin, *ibid.*, p. 97.  
<sup>14</sup>V. M. Ermachenko, *ibid.*, p. 104.  
<sup>15</sup>W. Heitler, The Quantum Theory of Radiation, Oxford, 1954.  
<sup>16</sup>L. V. Keldysh, Zh. Eksp. Teor. Fiz. 47, 1515 (1964) [Sov. Phys. JETP 20, 1018 (1965)].  
<sup>17</sup>I. B. Levinson, Zh. Eksp. Teor. Fiz. 65, 331 (1973) [Sov. Phys. JETP 38, 162 (1974)].  
<sup>18</sup>S. A. Bulgadaev, V. I. Kaplan, and I. B. Levinson, Zh. Eksp. Teor. Fiz. 70, 1550 (1976) [Sov. Phys. JETP 43, 808 (1976)].  
<sup>19</sup>A. Schawlow, transl. in: Lazery (Lasers), ed. by M. E. Zhabotinskiĭ and T. A. Shmaonov, IIL. 1963, p. 51.  
<sup>20</sup>S. Geschwind, G. E. Devlin, R. L. Cohen, and S. R. Chinn, Phys. Rev. 137, A1087 (1965).  
<sup>21</sup>M. Blume, R. Orbach, A. Kiel, and S. Geschwind, Phys. Rev. 139, A314 (1965).  
<sup>22</sup>N. A. Kurnit, I. B. Abella, and S. R. Hartmann, Physics of Quantum Electronics, McGraw Hill, New York, 1966, p. 267.  
<sup>23</sup>O. Anderson, in: Physical Acoustics, W. Mason, ed., (Russ. transl. Mir. 1968, p. 62).  
<sup>24</sup>F. Varsani, D. A. Wood, and A. L. Schawlow, Phys. Rev. Lett. 3, 544 (1959).  
<sup>25</sup>J. E. Rives and R. S. Meltzer, Phys. Rev. B 16, 1808 (1977).

Translated by J. G. Adashko

## Screening of charges and Friedel oscillations of the electron density in metals having differently shaped Fermi surfaces

A. M. Gabovich, L. G. Il'chenko, E. A. Pashitskiĭ, and Yu. A. Romanov

Physics Institute, Ukrainian Academy of Sciences

(Submitted 15 March 1978)

Zh. Eksp. Teor. Fiz. 75, 249-264 (July 1978)

Analytic and numerical integration methods are used to obtain the spatial distribution of the screened Coulomb potential of point charges in the interior and on the surface of metals having different Fermi-surface shapes. It is shown that in isotropic metals with quasi-two-dimensional or quasi-one-dimensional electron spectra the Friedel oscillations of the electron density decreases along normals to a cylindrical or plane Fermi surface, like  $r^{-2} \sin 2k_F r$  or  $r^{-1} \cos 2k_F r$ , respectively, and attenuate exponentially in perpendicular directions. Along the surface of an isotropic metal with a spherical Fermi surface, the Friedel oscillations decrease like  $r^{-5/2} \cos 2k_F r$ . In the Thomas-Fermi approximation, the screened charge potential in a homogeneous metal takes the form  $e^{-\kappa r}/r$  regardless of the shape of the Fermi surface, and along the surface of a semi-infinite metal it decreases in power-law fashion like  $r^{-3}$ . An expression is obtained for the potential energy of the charges near the surface of a metal. This expression, together with the image forces, describes the Friedel oscillations and the dipole-dipole interactions. The results explain, in particular, the experimental data on the ordering of adsorbed Sr and La films on the (112) faces of W and Mo single crystals.

PACS numbers: 71.45.Jp, 71.25.-3, 71.90.+q

### 1. INTRODUCTION

It is known that the steplike character of the Fermi distribution of the conduction electrons in metals leads to the appearance of the so-called Friedel oscillations of the screened Coulomb potential, which by virtue of the spherical Fermi surface over large distances from the charge,  $r \gg k_F^{-1}$  ( $k_F$  is the Fermi momentum,  $\hbar = 1$ ) decrease like  $r^{-3} \cos 2k_F r$ .<sup>[1,2]</sup> For the same reason, the Ruderman-Kittel-Kasuya-Yosida (RKKY) interaction between the magnetic moments of nuclei or paramagnetic impurities in an isotropic metal behaves asymptotically like  $r^{-3}$ .

The law governing the decrease of the Friedel oscillations depends, however, on the "dimensionality of the metal"  $d$ , i.e., on whether we are dealing with a bulky metal, with a film, or with a thin filament. Therefore even in the case of a three-dimensional isotropic electron spectrum, as shown by Adawi,<sup>[4]</sup> the perturbation  $\delta n$  of the electron density decreases like  $r^{-5/2} \cos 2k_F r$  at  $d=2$  and like  $r^{-2} \sin 2k_F r$  at  $d=1$ . If at the same time the electron spectrum is two-dimensional at  $d=2$  and one-dimensional at  $d=1$ , then the screened Coulomb potential decreases respectively like  $r^{-2} \sin 2k_F r$  (Ref.5) and  $r^{-1} \cos 2k_F r$ .<sup>[6]</sup>

On the other hand, as shown in Ref. 7, in a semi-infinite metal the behavior of the Friedel oscillations can be greatly influenced by the metal-vacuum interface, which alters the symmetry and effective dimensionality of the problem.

Finally, the character of the asymptotic behavior of the screened potential changes with the shape of the Fermi surface of the conduction electrons, as shown by Balkarev and Sandomirskii<sup>[8]</sup> with the penetration of a homogeneous electrostatic field into a metal as an example, and also in an analysis<sup>[7]</sup> of the indirect interaction of adsorbed atoms in the surface of a metal via the electron gas of the substrate.

In the present paper, on the basis of expressions for the electron polarization operator for different Fermi surfaces<sup>[9]</sup> we obtain, by analytic and numerical integration, the spatial distributions of the screened Coulomb potential of a point charge in the interior and on the surface of a metal. In Sec. 2 it is shown that in strongly anisotropic three-dimensional metals with cylindrical or spherical Fermi surfaces the Friedel oscillations, produced as a result of a root or logarithmic singularity of the polarization operator at a momentum transfer  $q=2k_F$ , decrease along the normals to the Fermi surfaces like  $1/r^2$  or  $1/r$ , respectively, and attenuate exponentially in the perpendicular directions. The indirect interaction between the magnetic moments via the conduction electrons of the metal takes in this case a similar form, in contrast to the RKKY formula.<sup>[3]</sup>

It is shown in Sec. 3, on the basis of an expression obtained in Ref. 10 for the Coulomb Green's function of an inhomogeneous system, that in the case of a spherical Fermi surface the law governing the decrease of the Friedel oscillations along the surface of the metal takes, by virtue of the symmetry of the problem, the form  $r^{-5/2}$ , as against  $r^{-3}$  obtained in Refs. 11 and 12 or in accord with the numerical calculations of Ref. 13. In the case of a semi-infinite metal with cylindrical or plane Fermi surface perpendicular to the metal-vacuum boundary, the electron-density oscillations decrease along the metal surface like  $r^{-2}$  or  $r^{-1}$ , and attenuate exponentially in the interior of the metal.

We obtain also an expression for the energy of interaction of two charges located near the surface of a metal, with account taken of the classical image forces; this expression describes both the dipole-dipole interaction and the Friedel oscillations, something that could not be done earlier.<sup>[14]</sup> The results point to a substantial role of the indirect interaction between the charged atoms via the collectivized electrons of the substrate metal, and make it possible in principle to explain the structure of monatomic adsorbed strontium and lanthanum films on the (112) face of tungsten and molybdenum single crystals.<sup>[15-18]</sup>

## 2. FRIEDEL OSCILLATIONS IN THE INTERIOR OF A METAL

It can be easily shown with the aid of the Maxwell material equation  $\text{div } \mathbf{D}=0$  and the nonlocal relation be-

tween the induction  $\mathbf{D}$  and the intensity  $\mathbf{E}$  of the electric field

$$D_i(\mathbf{r}) = \int d\mathbf{r}' \varepsilon_{ij}(\mathbf{r}, \mathbf{r}') E_j(\mathbf{r}'),$$

where  $\varepsilon_{ij}(\mathbf{r}, \mathbf{r}')$  is the dielectric tensor of a medium with spatial dispersion, the effects of static screening of a point charge  $Q(\mathbf{r}) = e\delta(\mathbf{r})$  in a metal with arbitrary Fermi-surface shape are described by the Fourier component of the potential  $\varphi(\mathbf{r})$  of the longitudinal field  $\mathbf{E} = -\nabla\varphi$ ; this component is of the form

$$\varphi(\mathbf{q}) = \frac{4\pi e}{q_i q_j \varepsilon_{ij}(\mathbf{q})}, \quad \varepsilon_{ij}(\mathbf{q}) = \delta_{ij} + 4\pi \kappa_{ij}(\mathbf{q}), \quad (2.1)$$

where  $\kappa_{ij}(\mathbf{q})$  is the tensor of the electronic polarizability of the metal.

We consider hereafter, besides the isotropic case, also strongly anisotropic metals with quasi-two-dimensional or quasi-one-dimensional electron spectra, when in practice only the transverse component  $\kappa_{\perp}$  or the longitudinal component  $\kappa_{\parallel}$  (relative to some axis  $z$ ) of  $\kappa_{ij}$  differs from zero. The screening is described for simplicity in the random-phase approximation (RPA), since the Fermi-liquid interaction between the electrons, at least within the framework of models such as Hubbard's,<sup>[19]</sup> does not influence the damping or the period of the Friedel oscillations (see Ref. 2).

### 2.1. Metal with spherical Fermi surface

The potential Coulomb energy of the charge in an isotropic metal with a spherical Fermi surface can be represented in the form

$$V(r) = e\varphi(r) = \frac{2e^2}{\pi} \int_0^{\infty} \frac{q^2 dq}{q^2 + 4\pi e^2 \Pi(q)} \frac{\sin qr}{qr}. \quad (2.2)$$

Here  $\Pi(q)$  is the static polarization operator of the electrons, given in the RPA by

$$\Pi(q) = \frac{q^2}{e^2} \kappa(q) = N(k_F) \left[ 1 + \frac{4k_F^2 - q^2}{4k_F q} \ln \left| \frac{q + 2k_F}{q - 2k_F} \right| \right], \quad (2.3)$$

where  $N(k_F) = m^* k_F / 2\pi^2$  is the state density per spin and  $m^*$  is the effective mass of the conduction electron.

It can be easily shown by double integration by parts<sup>[20]</sup> that the weak logarithmic singularity of (2.3) at the point  $q=2k_F$ , where  $d\Pi/dq|_{q=2k_F} = -\infty$ , leads to the appearance of singular terms of the type  $(q-2k_F)^{-1} \sin qr$  in the integrand of (2.2), so that in the region  $r \gg k_F^{-1}$  there appear long-range oscillations of the type  $r^{-3} \cos 2k_F r$ .

To determine the amplitude and phase of these oscillations it is necessary to calculate the screened potential  $V(r)$  for all values of  $r$ . To this end we used a computer to integrate numerically expression (2.3), which takes in dimensionless variables the form

$$v(\rho) = \frac{4}{\pi^2 \alpha \rho} \int_0^{\infty} s ds \sin s\rho \left/ \left[ s^2 + \frac{\alpha}{2} \left( 1 + \frac{1-s^2}{2s} \ln \left| \frac{s+1}{s-1} \right| \right) \right] \right. \quad (2.4)$$

where

$$v = V \frac{a_0^*}{e^2}, \quad \alpha = \frac{1}{\pi k_F a_0^*}, \quad \rho = 2k_F r, \quad s = \frac{q}{2k_F};$$

$a_0^* = 1/m^* e^2$  is the Bohr radius of the electron.

Figure 1 shows the dependence of the potential  $v(\rho)$  on  $\rho$  at  $\alpha = 1$ , obtained with the aid of the special method developed by Longman to integrate numerically oscillating functions.<sup>[21]</sup> It is seen that the Friedel oscillations set in already at  $\rho \sim 1$ , and in the region  $\rho \gg 1$  their envelope approaches a  $\rho^{-3}$  dependence (dashed curves). For comparison, the dash-dot curve in Fig. 1 shows also the form of the screened potential in the Thomas-Fermi approximation (TFA), which equals in our notation

$$v_{TF}(\rho) = \frac{4}{\pi^2 \alpha \rho} \int_0^\infty \frac{ds}{s} \frac{\sin sp}{1 + \alpha/s^2} = \frac{2}{\pi \alpha \rho} \exp\{-\rho \sqrt{\alpha}\}. \quad (2.5)$$

We note that a finite temperatures  $T \neq 0$  the smearing of the Fermi distribution functions makes the derivative  $d\Pi/dq$  finite as  $q \rightarrow 2k_F$  and equal to

$$\left. \frac{d\Pi}{dq} \right|_{q=2k_F} \approx \frac{m^*}{4\pi^2} \ln \frac{T}{E_F},$$

where  $E_F = k_F^2/2m^*$  is the Fermi energy of the electrons; the result is additional damping of the Friedel oscillations, with a characteristic length  $L_T = k_F/4\pi m^* T$ , in a accord with the law  $(r/L_T) \sinh^{-1}(r/L_T)$  (Ref. 4). At sufficiently low temperatures  $T \ll 0.1E_F$ , however, when  $L_T$  is much larger than the period  $\pi/k_F$  of the oscillations, this damping can be disregarded. For similar reasons we can neglect the loss of coherence of the Friedel oscillations on account of the scattering of the electrons by the impurities, inasmuch as in sufficiently pure metals the mean free path is  $l \gg \pi/k_F \sim 10^8$  cm.

## 2.2. Metal with cylindrical Fermi surface

In real metals one frequently encounters open Fermi surfaces of the slightly-corrugated-cylinder type.<sup>[22]</sup>

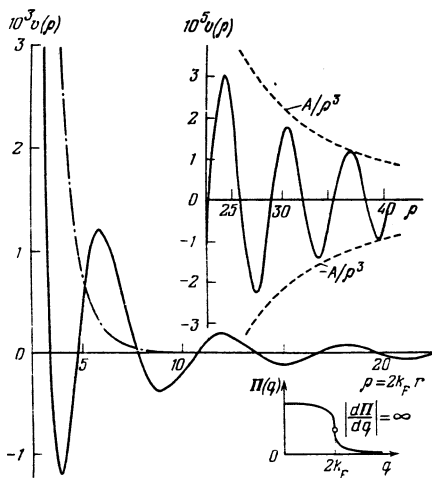


FIG. 1. Screened potential of a charge in the interior of a metal with a spherical Fermi surface: solid curve—random-phase approximation, dash-dot—Thomas-Fermi approximation. Top—asymptotic form of the Friedel oscillations, bottom—static polarization operator of electron gas:  $\alpha = 1/\pi k_F a_0^*$ ;  $A = 0.608$ .

We consider in this connection the model of a strongly anisotropic metal with a purely two-dimensional electron spectrum and with the symmetry axis of the cylindrical Fermi surface parallel to the  $z$  axis. The polarization operator  $\Pi(q_\perp) \equiv (q_\perp^2/e^2) \chi_\perp(q_\perp)$  takes in this case the form<sup>[9]</sup>

$$\Pi(q_\perp) = v_0 \operatorname{Re} \{1 - [1 - (2k_F/q_\perp)^2]^{1/2}\}, \quad (2.6)$$

where  $v_0 = m^* q_0/\pi^2$  is the two-dimensional state density,  $q_0$  is the length of the cylindrical section of the Fermi surface along the  $z$  axis, and  $q_\perp$  is the transverse momentum in the  $xy$  plane. The screened potential of the point charge reduces then, after integration with respect to  $q_z$ , to the form

$$v(\rho_\perp, \zeta) = \frac{2}{\pi \alpha} \int_0^\infty dt J_0(\rho_\perp t) \frac{\exp\{-\zeta[t^2 + \kappa \operatorname{Re}(1 - (1 - 1/t^2)^{1/2})]^{1/2}\}}{[t^2 + \kappa \operatorname{Re}(1 - (1 - 1/t^2)^{1/2})]^{1/2}}, \quad (2.7)$$

where

$$\rho_\perp = 2k_F R_\perp, \quad \zeta = 2k_F z, \quad t = q_\perp/2k_F, \quad \kappa = \pi e^2 v_0/k_F^2,$$

$J_0$  is a Bessel function, and  $R_\perp = (x^2 + y^2)^{1/2}$ .

Integrating (2.7) by parts and retaining the most singular terms of the form  $(t^2 - 1)^{-1/2}$ , we have at  $\rho_\perp \gg 1$  and  $\zeta \gg 1$

$$v(\rho_\perp, \zeta) \approx -\frac{\kappa \zeta \exp\{-\zeta(1 + \kappa)\}}{\pi \alpha (1 + \kappa)} \frac{\sin \rho_\perp}{\rho_\perp^2}. \quad (2.8)$$

Thus, the Friedel oscillations along the normal to the cylindrical Fermi surface decrease like  $R_\perp^{-2}$ , and attenuate exponentially along the  $z$  axis.

Figure 2 shows the results of a numerical integration of expression (2.7). We see that with increasing  $\rho_\perp$  the envelope of the oscillations acquires rapidly a  $\rho_\perp^{-2}$  dependence (dashed line). We note that if no account is taken of the root singularity in (2.7) under the assumption that  $\Pi(q_\perp) = v_0 = \text{const}$ , which corresponds to the

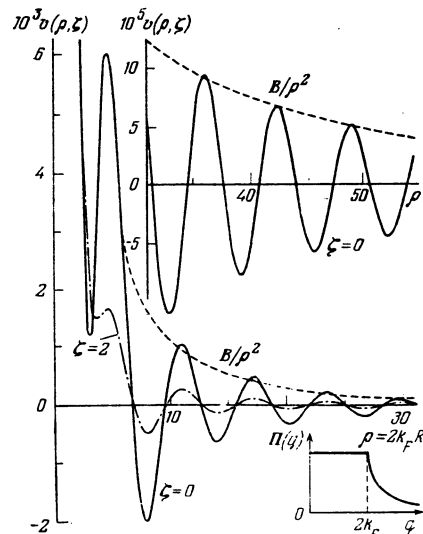


FIG. 2. Screened potential of a charge in the interior of a metal with a cylindrical Fermi surface in the RPA at  $\zeta = 0$  (solid curve) and  $\zeta = 2$  (dash-dot). Top—asymptotic curve with envelope  $B/\rho^2$  (dashed line), bottom—polarization operator of two-dimensional electron gas with root singularity at the point  $q_\perp = 2k_F$ ;  $\alpha = \kappa = 1$ ,  $B = 0.12$ .

TFA, the integral (2.7) simplifies and reduces to an expression of the type (2.5), from which it follows that notwithstanding the two-dimensional character of the electron spectrum, the screening of the charge, by virtue of the three-dimensionality of the metal, remains exponential just as in the isotropic case. On the other hand, in a two-dimensional metallic film the screening retains a power-law character in the TFA<sup>[5]</sup>:

$$v_{rr'}(R) \approx e^2 (a_0^*)^2 / 4R^2. \quad (2.9)$$

### 2.3. Metal with plane Fermi surface

A number of transition metals (W, Mo) are characterized by the presence of close-packed chains of atoms, so that in some direction the Fermi surface has nearly flat sections with negative curvature (see, e.g., Refs. 23 and 24). In this case the polarization operator  $\Pi(q_z) \equiv (q_z^2/e^2)\chi_{11}(q_z)$ , as shown by Afanas'ev and Kagan,<sup>[9]</sup> diverges logarithmically as  $T \rightarrow 0$  at the point  $q_z = 2k_F$  (the  $z$  axis is perpendicular to the Fermi planes). At arbitrary  $q_x$  we have for  $\Pi(q_z)$  (cf. Ref. 9)

$$\Pi(q_z) = v_F \frac{2k_F}{q_z} \ln \left| \frac{q_z + 2k_F}{q_z - 2k_F} \right|, \quad (2.10)$$

where  $v_F = m^* S_{\perp} / 4\pi^3 k_F$  is the one-dimensional density of the electronic states and  $S_{\perp} = \int dq_x dq_y$  is the area of the flat section of the Fermi surface.

Assuming isotropy of the spectrum in the  $xy$  plane, the expression for the screened potential takes in dimensionless variables, after integration with respect to  $q_{\perp}$ , the form

$$v(\zeta, \rho_{\perp}) = \frac{4}{\pi^2 \alpha} \int_0^{\infty} dt \cos t\zeta \cdot K_0 \left( \rho_{\perp} \left[ t^2 + \frac{\sigma}{2t} \ln \left| \frac{t+1}{t-1} \right| \right]^{1/2} \right), \quad (2.11)$$

where  $\sigma = 2\pi e^2 v_F / k_F^2$ ,  $t = q_z / 2k_F$ , and  $K_0$  is a MacDonald function. Integrating in (2.11) once by parts and retaining the most singular terms  $\sim |t-1|^{-1}$ , and recognizing that the electron spectrum is not quite one-dimensional or that the temperature is not finite, we arrive at the following asymptotic form of  $v(\zeta, \rho_{\perp})$  at  $\zeta \gg 1$  and  $\rho_{\perp} \gg 1$ :

$$v(\zeta, \rho_{\perp}) \approx -\frac{\sigma}{2\alpha} \left( \frac{2\rho_{\perp}}{\pi} \right)^{1/2} \frac{\exp\{-\rho_{\perp} (1/2 \sigma \ln U)^{1/2}\} \cos \zeta}{(1/2 \sigma \ln U)^{1/2} \zeta}, \quad (2.12)$$

where  $U = \min\{E_F/\varepsilon_{\perp}, E_F/T\}$  and  $\varepsilon_{\perp}$  is the transverse electron energy and characterizes the degree of corrugation of the flat Fermi surface.

As  $\rho_{\perp} \rightarrow 0$  expression (2.11) reduces to

$$v(\zeta, \rho_{\perp} \rightarrow 0) = -\frac{4}{\pi\alpha} \ln \rho_{\perp} \cdot \delta(\zeta) - \frac{2}{\pi^2 \alpha} \int_0^{\infty} dt \cos t\zeta \cdot \ln \left[ t^2 + \frac{\sigma}{2t} \ln \left| \frac{t+1}{t-1} \right| \right], \quad (2.13)$$

hence we get at  $\zeta \gg 1$  and  $\rho_{\perp} = 0$ , in place of (2.12) ( $\sigma \neq 0$ )

$$v(\zeta, 0) \approx \frac{2}{\pi\alpha \ln U} \frac{\cos \zeta}{\zeta}. \quad (2.14)$$

Figure 3 shows the plots of the screened potential  $v(\zeta, \rho_{\perp})$  calculated from (2.11) and (2.13). We see that at  $\zeta \gg 1$  the amplitude of the Friedel oscillations decreases slowly like  $\zeta^{-1}$ , in accord with (2.12) and (2.14).

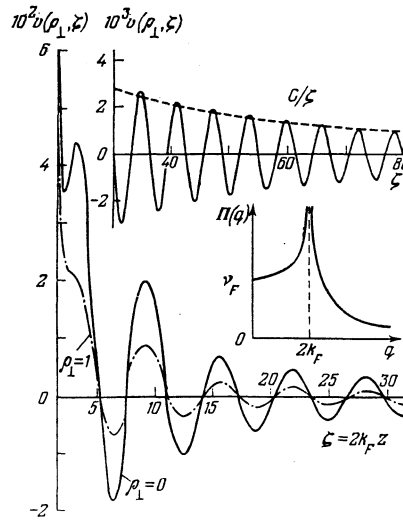


FIG. 3. Experimental potential of a charge in the interior of a metal with a flat Fermi surface in the RPA at  $\rho_{\perp} = 0$  (solid curve) and  $\rho_{\perp} = 1$  (dash-dot). Top—asymptotic Friedel oscillations with envelope  $C/\zeta$ ; center—polarization operator of one-dimensional electron gas with logarithmic singularity at the point  $q_z = 2k_F$ ;  $\alpha = \sigma = 1$ ;  $C = 0.84$ .

If we neglect in the expression for the screened potential the logarithmic singularity of the polarization operator (2.10) at  $q_z = 2k_F$  and put  $\Pi(q_z) = v_F = \text{const}$ , i.e., if we use the TFA, then we obtain an exponential charge screening similar to (2.5). Thus, if we disregard the Friedel oscillations, then in a three-dimensional metal consisting of one-dimensional conducting chains the attenuation of the Coulomb repulsion as a result of screening has the same character as in "solid" isotropic metal. Direct calculation in  $r$ -space with allowance for the discrete character of the ion chains<sup>[25]</sup> leads to a similar result:

$$v_{rr'}(r_n) \approx e^2 \exp\{-\lambda(r_n + b)\} / (r_n + b),$$

where  $b$  is the distance between chains,  $r_n$  are the locations of the ions, and  $\lambda$  is the screening constant, which is particularly long in quasi-one-dimensional compounds. At the same time, in an individual one-dimensional metallic chain there is no screening.<sup>[25]</sup>

Starting with the expression for the static paramagnetic susceptibility,<sup>[3]</sup> we can also show that in anisotropic metals the oscillating indirect interaction between the magnetic moments via the conduction electrons decreases with distance much more slowly (like  $R^{-2}$  or  $z^{-1}$ ) than in accord with the RKKY formula. Moreover, at sufficiently high degree of one-dimensionality of the electron spectrum, the logarithmic singularity of the polarization operator  $\Pi(q_z)$  at the point  $q_z = 2k_F$  can lead to instability of the ground paramagnetic state of the metal and to antiferromagnetic ordering accompanied by appearance of a static spin-density wave with a period  $L_s = \pi/k_F$  (Ref. 26).

To conclude the section, we note that the oscillating "tail" of the screened potential of a charged interstitial impurity in a metal matrix with a flat Fermi surface decreases in accord with the same law ( $\sim 1/r$ ) as the fields of the elastic deformations of the crystal.<sup>[27]</sup> Therefore

the structure of the ordered interstitial alloys (including hydrides of transition metals) should be determined in this case by the joint action of both factors—the elastic stresses and the Coulomb interaction of the impurities.

### 3. OSCILLATIONS OF ELECTRON DENSITY ON THE SURFACE OF A METAL. INTERACTION BETWEEN ADSORBED ATOMS

We proceed to consider the screening of charges near the surface of a semi-infinite metal. To describe the Coulomb interaction in such an inhomogeneous system, with account taken of the collective effects of screening and retardation, which are connected with the excitation of virtual plasma oscillations, we start with the temperature Green's function of a longitudinal self-consistent field  $D(\mathbf{r}, \mathbf{r}'; i\omega_n)$ , which satisfies the nonlocal Poisson equation<sup>[10]</sup>

$$\nabla_i^2 D(\mathbf{r}, \mathbf{r}'; i\omega_n) - 4\pi e^2 \int d\mathbf{r}'' \Pi(\mathbf{r}, \mathbf{r}''; i\omega_n) D(\mathbf{r}'', \mathbf{r}'; i\omega_n) = \delta(\mathbf{r} - \mathbf{r}'), \quad (3.1)$$

where

$$\Pi(\mathbf{r}, \mathbf{r}'; i\omega_n) = 2T \sum_{\mathbf{n}'} G(\mathbf{r}, \mathbf{r}'; i\epsilon_{\mathbf{n}'}) G(\mathbf{r}', \mathbf{r}; i(\epsilon_{\mathbf{n}'} - \epsilon_{\mathbf{n}'}))$$

is the polarization operator,  $G(\mathbf{r}, \mathbf{r}'; i\epsilon_n)$  is the temperature Green's function of the conduction electrons of the metal, while  $\omega_n = 2n\pi T$  and  $\epsilon_n = (2n+1)\pi T$  are the discrete even and odd "frequencies" ( $n=0, \pm 1, \pm 2, \dots$ ).

Equation (3.1) was solved in Ref. 10 for a three-layer of the insulator-metal-insulator type with account taken of the continuity of the function  $D$  and of its first derivative with respect to  $\mathbf{r}$  and  $\mathbf{r}'$  on the infinitesimally thin separation boundaries between the media. In the case of a semi-infinite metal, when the metal-layer thickness is  $L \rightarrow \infty$ , the potential electrostatic energy of two charges  $e_1$  and  $e_2$  located in the vacuum outside the metal at points  $\mathbf{r}_1$  and  $\mathbf{r}_2$  and at distances  $x_1$  and  $x_2$  from its surface (the  $x$  axis is perpendicular to the metal-vacuum interface, which coincides with the  $yz$  plane) can be represented in the form

$$W = -4\pi e_1 e_2 D(\mathbf{r}_1, \mathbf{r}_2; \omega_n = 0) + \frac{e_1 e_2}{|\mathbf{r}_1 - \mathbf{r}_2|} - 4\pi e_1 e_2 \int \frac{d^2 \mathbf{q}}{(2\pi)^2} \left[ D(\mathbf{q}, x_1 + x_2) - \frac{\exp\{-q|x_1 - x_2|\}}{2q} \right] e^{i\mathbf{q}\mathbf{r}} - \frac{1}{2} \sum_{i=1}^{\infty} 4\pi e_i^2 \int \frac{d^2 \mathbf{q}}{(2\pi)^2} D(\mathbf{q}, 2x_i), \quad (3.2)$$

where

$$D(\mathbf{q}, x) = \frac{e^{-q|x|}}{2q} \frac{1 - qa(\mathbf{q})}{1 + qa(\mathbf{q})}, \quad (3.3)$$

$$a(\mathbf{q}) = \frac{1}{\pi} \int_{-\infty}^{\infty} \frac{dk_{\perp}}{(k_{\perp}^2 + q^2) \epsilon(k_{\perp}, \mathbf{q})},$$

and  $\epsilon(k_{\perp}, \mathbf{q})$  is the static dielectric constant of the metal,

$$q = \{0, q_y, q_z\}, \quad R = |\mathbf{R}_1 - \mathbf{R}_2| = [(y_1 - y_2)^2 + (z_1 - z_2)^2]^{1/2}.$$

The last term in (3.2) describes the energy of attraction of the charges to the metal by the image forces due to the polarization (redistribution) of the electrons.

In the TFA, when  $a(\mathbf{q}) = (q^2 + \kappa_{TF}^2)^{-1/2}$ , this energy per charge is given by

$$W_i(x) = -\frac{e^2}{2} \int_0^{\infty} dq e^{-2qx} \frac{[q^2 + \kappa_{TF}^2]^{1/2} - q}{[q^2 + \kappa_{TF}^2]^{1/2} + q}, \quad (3.4)$$

where  $\kappa_{TF} = 2k_F \sqrt{\alpha}$  is the reciprocal Thomas-Fermi screening radius. At  $x > 0$  the integral (3.4) can be reduced by simple transformations to the form

$$W_i(x) = -\frac{e^2}{4x} \left\{ 1 + \frac{1}{(\kappa_{TF} x)^2} - \frac{\pi}{\kappa_{TF} x} [\mathbf{H}_1(2\kappa_{TF} x) - N_1(2\kappa_{TF} x)] + \pi [\mathbf{H}_0(2\kappa_{TF} x) - N_0(2\kappa_{TF} x)] \right\}, \quad (3.5)$$

where  $\mathbf{H}_0$  and  $\mathbf{H}_1$  are Struve functions, and  $N_0$  and  $N_1$  are Neumann functions.

At a sufficiently large distance from the metal surface, when  $x \gg \kappa_{TF}^{-1}$ , this yields

$$W_i(x) \approx -\frac{e^2}{4x} \left( 1 - \frac{1}{\kappa_{TF} x} \right). \quad (3.6)$$

The principal term in (3.6) corresponds to the classical image forces. At  $x \ll \kappa_{TF}^{-1}$ , on the other hand, we get from (3.5)

$$W_i(x) \approx -\frac{1}{2} e^2 \kappa_{TF} [1 + \frac{3}{2} \kappa_{TF} x \{ \ln(\kappa_{TF} x) + C - \frac{3}{8} \}], \quad (3.7)$$

where  $C = 0.5772 \dots$  is the Euler constant. The quantity  $W_i(0)$  is finite and corresponds to the exchange-correlation part of the energy of the interaction of the charge with the semi-infinite metal.<sup>[28]</sup> Expression (3.4) thus contains information both on the image forces at large distances from the metal surface and on the multiparticle exchange-correlation effects inside the metal.

The potential energy of interaction of two charges located at equal distances  $x_1 = x_2 = x$  from the metal surface is, according to (3.2) and (3.3)

$$W_{12}(\mathbf{R}, x) = -\frac{e_1 e_2}{2\pi} \int \frac{d^2 \mathbf{q}}{q} e^{i\mathbf{q}\mathbf{R}} \left[ \frac{1 - qa(\mathbf{q})}{1 + qa(\mathbf{q})} e^{-2qx} - 1 \right]. \quad (3.8)$$

At  $x \gg a(q)$ , when the main contribution to the integral (3.8) is made by small momentum transfers  $q \ll 1/a(\mathbf{q})$ , we obtain the well-known classical expression

$$W_{12} = -\frac{e_1 e_2}{(R^2 + 4x^2)^{3/2}} + \frac{e_1 e_2}{R}, \quad (3.9)$$

whence we get at  $R \gg x$  the asymptotic expression

$$W_{12} \approx 2e_1 e_2 x^2 / R^3, \quad (3.10)$$

which coincides with the result of Kohn and Lau<sup>[14]</sup> and differs by a factor of two from the energy of interaction of two dipoles.

If one charge ( $e_1$ ) is in vacuum at a distance  $x$  from the metal surface, and the other ( $e_2$ ) is located at a depth  $x'$  in the interior of the metal, the interaction energy is given by

$$W_{12}(\mathbf{R}, x, x') = 4\pi e_1 e_2 \int \frac{d^2 \mathbf{q}}{(2\pi)^2} D(\mathbf{q}, x, x') e^{i\mathbf{q}\mathbf{R}}, \quad (3.11)$$

where

$$D(\mathbf{q}, x, x') = e^{-q|x|} \frac{a(\mathbf{q}, x')}{1 + qa(\mathbf{q})}, \quad (3.12)$$

$$a(\mathbf{q}, x') = \frac{1}{\pi} \int_{-\infty}^{\infty} \frac{\cos k_{\perp} x' dk_{\perp}}{(k_{\perp}^2 + q^2) \epsilon(k_{\perp}, \mathbf{q})}.$$

### 3.1. Semi-infinite metal with spherical Fermi surface

The dimensional potential interaction energy  $w = W_{12} a_0^* / e^2$  of two identical point charges ( $e_1 = e_2 = e$ ), one of which is on the surface of an isotropic metal ( $x = 0$ ) and the other is in its interior, is according to (3.11) and (3.12)

$$w(\rho, 0, \xi') = \frac{2}{\pi \alpha} \int_0^\infty t dt J_0(\rho t) \frac{h(t, \xi')}{1 + th(t, 0)}, \quad (3.13)$$

where

$$h(t, \xi') = \frac{2}{\pi} \int_0^\infty ds \cos \xi' s \times \left\{ s^2 + t^2 + \frac{\alpha}{2} \left[ 1 + \frac{1-s^2-t^2}{2(s^2+t^2)^{1/2}} \ln \left| \frac{1+(s^2+t^2)^{1/2}}{1-(s^2+t^2)^{1/2}} \right| \right] \right\}^{-1};$$

$$s = k_\perp / 2k_F, \quad t = q / 2k_F, \quad \rho = 2k_F R, \quad \xi' = 2k_F x'.$$

By integrating (3.13) twice by parts we easily obtain the following expressions for the interaction between the charges over the surface ( $\xi' = 0$ ) and in the interior of the metal ( $\rho = 0$ ) at large distances:

$$w(\rho, 0, 0) \approx \frac{8}{(2\pi)^{1/2} (2+\alpha)^2} \frac{\sin(\pi/4 - \rho)}{\rho^{3/2}}, \quad \rho \gg 1; \quad (3.14)$$

$$w(0, 0, \xi') \approx \frac{4}{(2+\alpha)^2} \frac{\cos \xi'}{(\xi')^2}, \quad \xi' \gg 1. \quad (3.15)$$

Figure 4 shows plots of  $w(\rho, 0, 0)$  against  $\rho$  and of  $w(0, 0, \xi')$  against  $\xi'$  as calculated from (3.13). It is easily seen that the oscillations of  $w(\rho, 0, 0)$  rapidly acquire the asymptotic  $\rho^{-5/2}$  dependence (upper dashed curve) and do not agree with the  $\rho^{-3}$  predicted by Grimley and Walker<sup>[11]</sup> (lower dashed curve).

In the TFA, expression (3.13) for a semi-infinite metal reduces to

$$w_{TF}(\rho, 0, \xi') = \frac{2}{\pi \alpha} \int_0^\infty t dt J_0(\rho t) \frac{\exp\{-\xi'(t^2 + \alpha)^{1/2}\}}{t + (t^2 + \alpha)^{1/2}}. \quad (3.16)$$

In the particular case  $\rho = 0$  the integral in (3.16) can be calculated exactly:

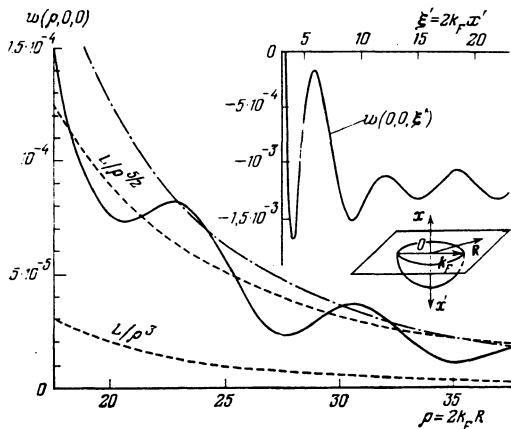


FIG. 4. Screened potential of a charge on the surface of a metal with a spherical Fermi surface: solid curve—RPA, dash-dot—TFA, dashed curves—dependences of the type  $w \propto L/\rho^{3/2}$  and  $L/\rho^3$ ;  $L = 0.16$ . Top—dependence of the potential on the depth of penetration  $\xi'$  into the metal.

$$w_{TF}(0, 0, \xi') = \frac{2}{\pi \alpha \xi'} \left\{ \exp(-\xi' \sqrt{\alpha}) \left[ 1 + \frac{2}{\xi' \sqrt{\alpha}} + \frac{2}{\alpha (\xi')^2} \right] - K_2(\xi' \sqrt{\alpha}) \right\}. \quad (3.17)$$

It follows from (3.17) that at large distances ( $\xi' \gg 1$ ) the screened Coulomb potential in TFA decreases in the interior of the metal like  $\exp(-\xi' \sqrt{\alpha})/\xi'$ , and this coincides with the solution (2.5) for a homogeneous metal.

At the same time, the presence of other terms in (3.17) is connected with the diffraction of the electrons by the metal-vacuum interface. On the metal surface ( $\xi' = 0$ ) we get, accurate to the principal terms [cf. (2.9)],

$$w_{TF}(\rho, 0, 0) \approx \frac{1}{\alpha \rho^3} \int_0^\infty J_2(u) du = \frac{\text{const}}{\rho^3}. \quad (3.18)$$

The dash-dot curve in Fig. 4 is a plot of  $w_{TF}(\rho, 0, 0)$  calculated with a computer in accord with formula (3.16) at  $\xi' = 0$ .

### 3.2. Semi-infinite metal with cylindrical Fermi surface

Consider the potential of a charge near the surface of a metal with a cylindrical Fermi surface whose symmetry axis is parallel to the  $x$  axis (see Fig. 5). Using expression (2.6) for the polarization operator, we reduce (3.11) to the form

$$w(\rho, 0, \xi') = \frac{2}{\pi \alpha} \int_0^\infty t dt J_0(\rho t) \frac{\exp\{-\gamma(t) \xi'\}}{t + \gamma(t)}, \quad (3.19)$$

where

$$\gamma(t) = [t^2 + \kappa \operatorname{Re}(1 - (1 - 1/t^2)^{1/2})]^{1/2}. \quad (3.20)$$

Integrating (3.19) by parts and retaining the most singular terms  $\propto (t^2 - 1)^{-1/2}$ , we obtain at  $\rho \gg 1$  and  $\xi' \gg 1$

$$w(\rho, 0, \xi') \approx -\frac{\kappa \xi' \exp\{-\xi'(1+\kappa)^{1/2}\} \sin \rho}{\pi \alpha (1+\kappa)^{1/2} [1 + (1+\kappa)^{1/2}] \rho^2}. \quad (3.21)$$

Figure 5 shows a plot of  $w(\rho, 0, \xi')$  against  $\rho$ , obtained by numerical integration for different values of  $\xi'$ .

In the TFA, expression (3.19) agrees, when the substitution  $\kappa \rightarrow \alpha$  is made, with expression (3.16), so that the results (3.17) and (3.18) are valid in this case, too.

We consider now in greater detail the question of two

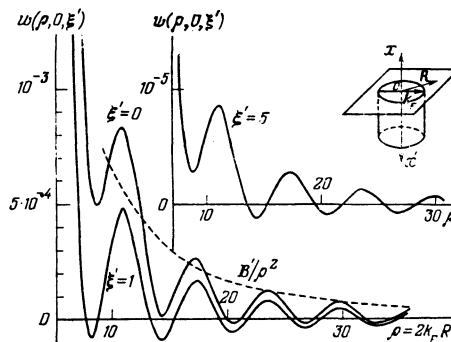


FIG. 5. Screened potential in RPA on the surface of a metal with a cylindrical Fermi surface perpendicular to the metal-vacuum interface, for different values of the penetration depth  $\xi'$ ;  $\alpha = \kappa = 1$ ;  $B' = 0.066$ .

### 3.3. Semi-infinite metal with flat Fermi surface

We proceed to the study of Friedel oscillations on the surface of a metal with flat sections of the Fermi surface. The geometry of the problem is shown in the insert of Fig. 7. We confine ourselves to a derivation of the dependences of the screened Coulomb potential on the coordinates  $y$  and  $z$  along the surface. The dimensionless potential of the charge reduces, according to (3.11) and (3.12) with (2.10) taken into account, to the form

$$w(\zeta, \eta, 0) = \frac{16}{\pi^2 \alpha \sigma \eta} \int_0^\infty dt t \cos \zeta t \ln^{-1} \left| \frac{t+1}{t-1} \right| \{tK_1(\eta t) - \tau K_1(\eta \tau)\}, \quad (3.23)$$

where

$$\tau(t) = \left[ t^2 + \frac{\sigma}{2t} \ln \left| \frac{t+1}{t-1} \right| \right]^{1/2},$$

$$\eta = 2k_F y, \quad t = q_z / 2k_F, \quad \zeta = 2k_F z.$$

Integrating by parts and retaining the most singular terms  $\sim |t-1|^{-1}$ , and taking into account the fact that the temperature or the transverse energy of the electrons is finite, we obtain the following asymptotic expression at  $\zeta \gg 1$  and  $\eta \gg 1$ :

$$w(\zeta, \eta, 0) \approx \frac{2\sigma}{\alpha(2\pi\eta)^{3/2}} \frac{\exp\{-\eta^{1/2} \sigma \ln U\} \cos \zeta}{(\zeta \sigma \ln U)^{3/2}}. \quad (3.24)$$

It is easy to verify that the damping is exponential also in the interior of the metal [cf. (2.12)]. On the other hand, as  $\eta \rightarrow 0$  it follows from (3.23) that

$$w(\zeta, \eta \rightarrow 0, 0) = -\frac{8}{\pi \alpha} \ln \eta \delta(\zeta) + \frac{8}{\pi^2 \alpha \sigma} \int_0^\infty dt t \cos \zeta t \ln^{-1} \left| \frac{t+1}{t-1} \right| \times \left( t^2 \ln \frac{t}{2} - \tau^2 \ln \frac{\tau}{2} \right). \quad (3.25)$$

Integrating (3.25) by parts we obtain in place of (3.24), in analogy with foregoing, at  $\zeta \gg 1$  and  $\eta = 0$ ,

$$w(\zeta, 0, 0) \approx \frac{2}{\pi \alpha} \frac{\cos \zeta}{\zeta}. \quad (3.26)$$

Figure 7 shows a plot of  $w(\zeta, \eta, 0)$  against  $\zeta$  and  $\eta$ , obtained by numerical integration starting with formulas (3.23) and (3.25). It follows from Fig. 7 that the screened Coulomb potential decreases slowly along the surface of the metal in the direction of the  $z$  axis, forming a potential relief of alternating sign, which is particularly deep at  $\eta = 0$  (the depth of the negative minima reaches  $|W_{\min}| \sim 10^{-2}$  Ry).

The coordinate dependence of the screened Coulomb potential on the surface of a metal with flat sections of the Fermi surface takes in the TFA, according to (3.23), the form

$$w_{TF}(\zeta, \eta, 0) = \frac{4}{\pi \alpha \sigma} \left\{ (\zeta^2 + \eta^2)^{-\eta} - \left( \frac{2}{\pi} \right)^{1/2} \sigma^{1/2} (\zeta^2 + \eta^2)^{1/2} K_{1/2}(\sigma^{1/2} (\zeta^2 + \eta^2)^{1/2}) \right\}. \quad (3.27)$$

At large distances from the charge, when  $\zeta \gg 1$  and (or)  $\eta \gg 1$ , the potential  $w_{TF} \approx 4/\pi \alpha \sigma \rho^3$  just as for metals with

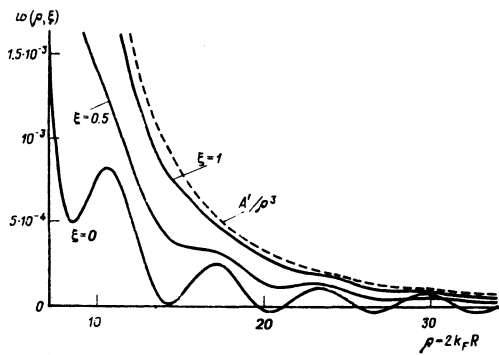


FIG. 6. Interaction energy of two charges located at different distances  $\xi$  from the surface of a metal with a cylindrical Fermi surface. Dashed curve—dipole-dipole interaction of the type  $A'/\rho^3$ ;  $A' = 2.70$ ;  $\alpha = \kappa = 1$ .

charges in vacuum at a distance  $x \gg \kappa_{TF}^{-1}$  from the surface of the metal, and show that in the RPA, at large distances between the charges, the dipole-dipole repulsion (3.10) predominates. For example, in the case of a metal with a cylindrical Fermi surface the energy of interaction of the charges according to (3.8), with allowance for (3.20), is

$$w(\rho, \xi) = \frac{1}{\pi \alpha} \int_0^\infty dt J_0(\rho t) \left[ e^{-2\eta} \frac{t - \tau(t)}{t + \tau(t)} + 1 \right]. \quad (3.22)$$

Figure 6 shows the results of a numerical calculation by formula (3.22). With increasing  $\xi = 2k_F x$ , i.e., with increasing distance between the charges and the metal surface, the Friedel oscillations become smoothed out and the dependence of the interaction energy  $w(\rho, \xi)$  on  $\rho$  tends to the  $\rho^{-3}$  law typical of the dipole-dipole repulsion. Consequently, it becomes possible to describe with the aid of (3.2) both the Friedel oscillations of a screened Coulomb potential and the direct dipole-dipole interaction of charges on the surface of a metal; this could not be done heretofore.<sup>[14]</sup>

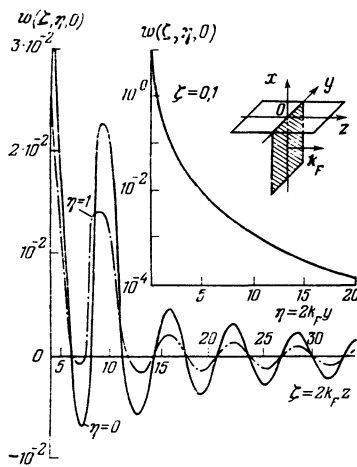


FIG. 7. Screened potential of a charge on the surface of a metal with a flat Fermi surface perpendicular to the metal—vacuum interface; below—Friedel oscillations along the  $z$  axis at  $\eta = 0$  (solid curve) and  $\eta = 1$  (dash-dot), top—fast falloff along the  $y$  axis at  $\xi = 0.1$ ;  $\alpha = \sigma = 1$ .

spherical and cylindrical Fermi surfaces.

The analytic results obtained in this section, together with the numerical calculations, show that the character of the Friedel oscillations of the electron density on the surface of the metal depends substantially on the shape of its Fermi surface. In the case of a metal with a spherical Fermi surface, the Friedel oscillations along the metal-vacuum interface decrease according to (3.14) more slowly ( $\sim R^{-5/2}$ ) than in the interior, but the minima of the potential energy are shallow and nowhere do they land in the region of negative values (Fig. 4).

On the surfaces of metals with cylindrical and flat Fermi surfaces, the Friedel oscillations attenuate according to (3.20), (3.24), and (3.26) like  $R^{-2}$  and  $z^{-1}$ , respectively. At definite distances  $R$  and  $z$  the potential energy of the interaction of like charges becomes negative (Figs. 5 and 7), meaning attraction.

The presence of such negative minima explains qualitatively the results of experiments<sup>[15-18]</sup> in which a peculiar pattern of ordering of monatomic La and Sr films on the anisotropic (112) faces of W and Mo single crystals was observed, with close-packed chains of W and Mo atoms disposed along the  $[\bar{1}\bar{1}1]$  crystallographic direction. As a result, the electron Fermi surface has almost-flat sections perpendicular to the  $[\bar{1}\bar{1}1]$  direction (see Refs. 23 and 24). When Sr and La is sputtered on the (112) face of W, monatomic films are produced with a primitive structure  $p(1 \times 7)$  (see Refs. 15-17), so that the equilibrium distance between the adsorbed atoms along the chains is equal to  $z_0 = 7a_2 \approx 19.2 \text{ \AA}$ , where  $a_2$  is the distance between the W atoms in the chain. When Sr is sputtered on the (112) face of Mo, at low concentrations of the adsorbed atoms,  $n_a < 10^{14} \text{ cm}^{-2}$ , a  $p(1 \times 9)$  structure is produced with  $z_0 = 9a_2 \approx 24.6 \text{ \AA}$ , and at larger  $n_a$  there is produced a structure  $p(1 \times 5)$  with  $z_0 = 5a_2 \approx 13.7 \text{ \AA}$  (Ref. 18). If it is assumed that for the Sr and La films on W the equilibrium distance  $z_0$  between the adsorbed atoms corresponds to the position of the second negative minimum of the screened potential at the point  $z_{\text{min}}^{(2)} \approx 12.8$  or  $z_{\text{min}}^{(2)} \approx 6.4k_F^{-1}$  (see Fig. 7), and it is recognized that for W in the  $[\bar{1}\bar{1}1]$  direction the Fermi momentum is  $k_F \approx 0.41 \text{ \AA}^{-1}$  (Ref. 23), we obtain the estimate  $z_0 \approx 15.6 \text{ \AA}$ , which is close to  $6a_2$ . In the case of Sr films on Mo, when  $k_F \approx 0.46 \text{ \AA}^{-1}$  (Ref. 24), the second and third minima of the interaction potential are at distances  $z_{\text{min}}^{(2)} \approx 13.8 \text{ \AA}$  and  $z_{\text{min}}^{(3)} \approx 20.6 \text{ \AA}$ , which corresponds to  $z_0 = 5a_2$  and  $z_0 = 7.5a_2$ .

We see that fair agreement is observed between the theoretical and experimental values of  $z_0$ , even though the shapes of the real Fermi surfaces of W and Mo differ substantially from flat. The indirect interaction be-

tween the adsorbed atoms via the conduction electrons of the substrate metal can thus play an important role in the ordering of adsorbed films.

In conclusion, we are grateful to V. K. Medvedev, A. G. Naumovets, V. L. Pokrovskii, Yu. G. Ptushinskiĭ, P. M. Tomchuk, and G. V. Uĭmin for useful discussions of the results.

- <sup>1</sup>J. S. Langer and S. H. Vosko, *J. Phys. Chem. Solids* **12**, 196 (1959).
- <sup>2</sup>H. R. Leribaux and M. H. Boon, *Phys. Rev. B* **11**, 2412 (1975).
- <sup>3</sup>R. M. White, *Quantum Theory of Magnetism*, McGraw, 1970.
- <sup>4</sup>I. Adawi, *Phys. Rev.* **146**, 379 (1966).
- <sup>5</sup>E. Canel, M. P. Matthews, and R. K. P. Zia, *Phys. Kondens. Mater.* **15**, 191 (1972).
- <sup>6</sup>A. K. Das, *Solid State Commun.* **15**, 475 (1974).
- <sup>7</sup>A. M. Gabovich and E. A. Pashitskiĭ, *Ukr. Fiz. Zh.* **20**, 1742 (1975); *Fiz. Tverd. Tela (Leningrad)* **18**, 377 (1976) [*Sov. Phys. Solid State* **18**, 220 (1976)].
- <sup>8</sup>Yu. I. Balkareĭ and V. B. Sandomirskiĭ, *Zh. Eksp. Teor. Fiz.* **54**, 808 (1968) [*Sov. Phys. JETP* **27**, 434 (1968)].
- <sup>9</sup>A. M. Afanas'ev and Yu. Kagan, *Zh. Eksp. Teor. Fiz.* **43**, 1456 (1962) [*Sov. Phys. JETP* **16**, 1030 (1963)].
- <sup>10</sup>Yu. A. Romanov, *Zh. Eksp. Teor. Fiz.* **47**, 2119 (1964) [*Sov. Phys. JETP* **20**, 1424 (1965)]; Author's Abstract of Candidate's Dissertation, Gor'kii, 1966.
- <sup>11</sup>T. B. Grimley and S. M. Walker, *Surf. Sci.* **14**, 395 (1969).
- <sup>12</sup>I. Rudnick, *Phys. Rev. B* **5**, 2863 (1972).
- <sup>13</sup>J. W. Gadzuk, *Solid State Commun.* **5**, 743 (1967).
- <sup>14</sup>W. Kohn and K. -H. Lau, *Solid State Commun.* **18**, 553 (1976).
- <sup>15</sup>V. K. Medvedev and A. I. Yakivchuk, *Ukr. Fiz. Zh.* **20**, 1900 (1975).
- <sup>16</sup>V. K. Medvedev, V. N. Pogoreliĭ, and A. I. Yakivchuk, *Pis'ma Zh. Eksp. Teor. Fiz.* **24**, 489 (1976) [*JETP Lett.* **24**, 449 (1976)].
- <sup>17</sup>Yu. S. Vedula, V. K. Medvedev, A. G. Naumovets, and V. N. Pogoreliĭ, *Ukr. Fiz. Zh.* **22**, 1826 (1977).
- <sup>18</sup>V. K. Medvedev and I. N. Yakovkin, *Fiz. Tverd. Tela (Leningrad)* **20**, 928 (1978) [*Sov. Phys. Solid State* **20**, 537 (1978)].
- <sup>19</sup>K. S. Singwi, A. Sjölander, M. P. Tosi, and R. Land, *Phys. Rev. B* **1**, 1044 (1970).
- <sup>20</sup>W. A. Harrison, *Pseudopotentials in the Theory of Metals*, Benjamin, 1966.
- <sup>21</sup>J. M. Longman, *Proc. Cambridge Philos. Soc.* **52**, 764 (1956); *Mathematics of Computation* **14**, 53 (1960).
- <sup>22</sup>I. M. Lifshitz, M. Ya. Azbel', and M. I. Kaganov, *Elektronnaya teoriya metallov (Electron Theory of Metals)*, Nauka, 1971.
- <sup>23</sup>R. F. Girvan, A. V. Gold, and R. A. Phillips, *J. Phys. Chem. Solids* **29**, 1485 (1968).
- <sup>24</sup>V. V. Boiko and V. V. Gasparov, *Zh. Eksp. Teor. Fiz.* **61**, 2362 (1971) [*Sov. Phys. JETP* **34**, 1266 (1972)].
- <sup>25</sup>D. Davis, *Phys. Rev. B* **7**, 129 (1973).
- <sup>26</sup>A. W. Overhauser, *Phys. Rev.* **128**, 1437 (1962).
- <sup>27</sup>H. Wagner and H. Horner, *Adv. Phys.* **23**, 587 (1974).
- <sup>28</sup>J. Appelbaum, *Surface Physics of Materials*, vol. 1, Academic Press, New York-London, 1975, pp. 79-119.

Translated by J. G. Adashko